

# Nickel Ammonium Sulfate Crystal Growth Rates in Aqueous Solution

John W. Mullin<sup>1</sup> and Mohamed M. Osman<sup>2</sup>

Department of Chemical Engineering, University College London, Torrington Place, London WC1E 7JE, England

**Growth rates of the two most important crystallographic faces (110) and (001) of nickel ammonium sulfate were measured and compared with overall mass deposition rates on the whole crystal. The "order" of the crystal growth process, with respect to concentration driving force, appeared to be strongly temperature dependent, increasing from about 1.2 to 1.7 over the range 15–35°C for the (110) face. The surface-reaction controlled growth rate was unaffected by solution velocity. The growth of the (001) face at 25°C was approximately second order.**

This work is part of a study on the precipitation kinetics of nickel ammonium sulfate (nickel sulfate + ammonium sulfate) in aqueous solution. Several basic physical properties of this nickel ammonium sulfate–water system (including density, viscosity, and refractive index) have been reported (5).

Nickel ammonium sulfate is a member of the isomorphous Tutton salts with the general formula  $M_2^{II}M^{II}(SO_4)_2 \cdot 6H_2O$ . The double salt hexahydrate (mol wt = 396) is easily precipitated by mixing aqueous solutions of nickel and ammonium sulfates in stoichiometric proportions. The crystals, which normally crystallize from aqueous solution as well-formed prisms, belong to the monoclinic system. The predominant crystal faces are (110) and (001), but others such as (011) and (201) are often clearly seen (Figure 1).

The solubility of nickel ammonium sulfate in water over the temperature range  $20^\circ < 0^\circ < 60^\circ\text{C}$  may be represented by the equation

$$c^* = 0.053 + 0.0018\theta + 0.000017\theta^2 \quad (1)$$

Other relevant properties include crystal density,  $\rho_c = 1923 \text{ kg/m}^3$ , density of saturated solution at  $20^\circ\text{C} = 1050 \text{ kg/m}^3$ , viscosity of saturated solution,  $\eta_s = 1.2 \times 10^{-3} \text{ N sec/m}^2$ .

## Growth Rate Measurements

The linear crystal growth rates of the predominant (110) and (001) faces were measured by a technique previously described (1–3). It would have been extremely difficult to measure the growth rates of the minor faces, such as (011) and (201), by this method since these are small in area compared with the major faces (Figure 1). No distinction is made here between faces with respect to the crystallographic axes. In other words, (110) signifies any one of the four faces (110), ( $\bar{1}\bar{1}0$ ), ( $\bar{1}10$ ), and (110); (001) signifies any one of the two faces (001) or (00 $\bar{1}$ ) (Figure 1).

Nickel ammonium sulfate was prepared by mixing stoichiometric quantities of nickel sulfate and ammonium sulfate solutions prepared from recrystallized salts and deionized water. The crystalline product formed was subsequently purified by recrystallization from water. A carefully grown seed crystal (4–5 mm in size) was mounted

with a nitrocellulose-based water-repellent adhesive (Durofix) on the end of a 1-mm diam. tungsten wire. The adhesive was allowed to dry in a vacuum oven for several hours before the mounted crystal was used.

The crystal was dipped into deionized water to remove any traces of impurities attached to the crystal surface and then introduced into a glass cell through which solution flowed at the required temperature. The washing process removed the sharp edges and corners from the crystal so that it was allowed to grow for at least 15 min before any actual measurements were started. The chosen face was observed with a traveling microscope reading to  $\pm 0.01 \text{ mm}$ , and its growth rate was determined.

Solution samples were taken before and after each run, and their concentration was measured. The mean driving force  $\Delta c$  was taken as the difference between the mean of the initial and final concentrations and the equilibrium saturation concentration  $c^*$  at the working temperature. As the increase in mass of the crystal was small compared with the mass of solute present in solution,  $\Delta c$  effectively remained constant.

## Linear Growth Rates of (110) Faces

Growth rates of the (110) faces were measured at three temperatures:  $15^\circ$ ,  $25^\circ$ , and  $35^\circ\text{C}$ . The concentration driving force  $\Delta c$  was varied from about 0.002 to 0.017 kg of hydrated NAS/kg of free water, and the flow of solution past the stationary crystal was changed alternately between the two chosen velocities of 60 and 270 mm/sec. Several runs were carried out at these temperatures, each lasting for about 4 hr or more to determine whether the growth rate (perpendicular to the face) remained constant with time. Under the given conditions, no apparent change in the growth rate could be detected.

The results are shown in Figure 2. As expected the growth rate increased with both supersaturation and temperature. No growth could be detected at  $\Delta c < 0.003$ ; similar limiting concentration driving forces have been noted for other salts, including ammonium and potassium alums, dihydrogen phosphates, and sulfates (7–4). The growth rate appeared to be independent of solution velocity and was confirmed by more detailed experiments (not recorded here) with velocities ranging down to 16 mm/sec.

When the data in Figure 2 are replotted on logarithmic coordinates (not shown here) straight-line correlations may be made for each operating temperature, and the results may be expressed in terms of the linear growth rate  $v$  and supersaturation  $\Delta c$  by a relationship of the form

$$v \propto (\Delta c)^g \quad (2)$$

where  $g$  is the "order" of the growth process. The significance of this term is explained fully elsewhere (2). The data may be correlated by

$$15^\circ\text{C}: v_{(110)} = 5.93 \times 10^{-6} (\Delta c)^{1.19} \quad (3)$$

$$25^\circ\text{C}: v_{(110)} = 1.86 \times 10^{-5} (\Delta c)^{1.36} \quad (4)$$

$$35^\circ\text{C}: v_{(110)} = 1.65 \times 10^{-4} (\Delta c)^{1.73} \quad (5)$$

<sup>1</sup> To whom correspondence should be addressed.

<sup>2</sup> Present address, Department of Chemical Engineering, University of Cairo, Cairo, Egypt.

It is important to emphasize that these equations may only be considered to apply within the concentration range studied, viz.,  $0.004 < \Delta c < 0.014$ . Equations 3–5 show the significant change in the "order" of growth (from 1.19 to 1.73) as the temperature is increased from 15° to 35°C. Furthermore, the increase in the exponent on  $\Delta c$  appears to be more rapid in the higher temperature range. These results tend to suggest that surface integration is the more dominant process in the growth of nickel ammonium sulfate hexahydrate crystals under the conditions used in this study.

The linear growth rates  $v$  as measured above can be transformed into mass-transfer or growth rate coefficients,  $K_G$ , by the equation

$$v = \frac{K_G}{\rho_c} (\Delta c)^g \quad (6)$$

The mass-transfer coefficient can also be related to the temperature by the Arrhenius equation which can, for this purpose, be written

$$\ln K_G = \ln B - E/RT \quad (7)$$

An estimate of the activation energy for growth,  $E_G$ , can be obtained from Equation 7 by plotting  $\log K_G$  vs.  $T^{-1}$ . Over the driving force range  $\Delta c = 0.003$  to 0.013, the activation energy increases from about 8 to 38 kJ/mol.

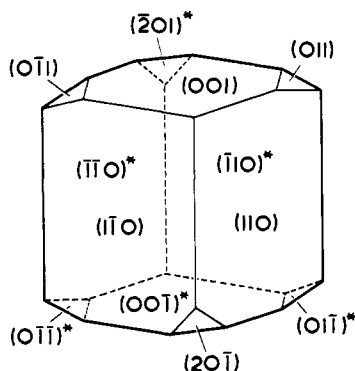


Figure 1. Nickel ammonium sulfate hexahydrate crystal (monoclinic) (\*, concealed faces)

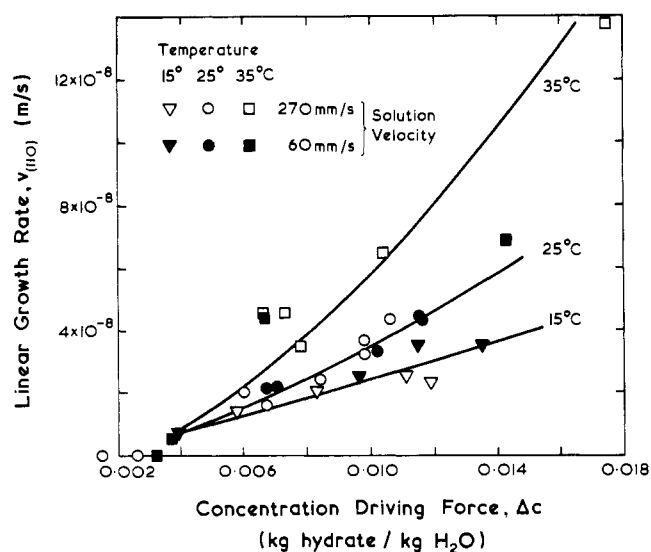


Figure 2. Effect of temperature and solution velocity on (110) face growth rates of nickel ammonium sulfate hexahydrate

This method of analysis is only strictly applicable when the exponent  $g$  of  $\Delta c$  is independent of temperature. In the present case of the (110) faces of nickel ammonium sulfate, however, the exponent increases with temperature (Equations 3–5) which means that the activation energy is also temperature dependent. A similar effect was reported for potash alum (3).

#### Linear Growth Rates of (001) Faces

Growth rates of the (001) faces of nickel ammonium sulfate were measured at one temperature (25°C) with concentration driving forces ranging from about 0.002 to 0.011 kg of hydrated NAS/kg of free water. Three solution flow rates (60, 180, and 270 mm/sec) were used to investigate the effect of velocity on the face growth rates.

The results are shown in Figure 3. As in the case of the (110) faces, no growth could be detected for  $\Delta c < 0.003$ , and solution velocity had no significant effect. A fair amount of scatter occurs, but this is perhaps not unexpected because the (001) faces are frequently bounded by the small, rapidly growing (201) faces, and these tend to interfere with the (001) growth. When these data are replotted on a log-log basis (not shown here), the best straight line is represented by

$$v_{(001)} = 6.01 \times 10^{-4} (\Delta c)^{2.04} \quad (8)$$

over the range of concentration  $0.003 < \Delta c < 0.011$ , i.e.,  $1.03 < S < 1.10$ .

On comparing the data for 25°C in Figures 2 and 3, for driving forces  $\Delta c > 0.005$ , the (001) growth rates are faster than the (110). This is in agreement with the well-known generalization that small faces grow faster than large; the higher integration rate on the (001) face most probably is due to the higher reticular density, in accordance with the Bravais rule (2).

#### Overall Mass Deposition Rates

Overall mass deposition rates on single crystals of nickel ammonium sulfate at 25°C were determined by a weighing technique. The apparatus and procedure were the same as those for the linear growth measurements except for a modification to the tungsten wire on which the crystal was mounted. This was made detachable to facilitate weighing. The crystals used ranged from about 0.1 to 1 gram, and their masses were measured to  $\pm 0.0001$  gram.

Supersaturations up to  $\Delta c \sim 0.014$  ( $S \sim 1.4$ ) were used and two solution velocities (60 and 270 mm/sec). The results are plotted in Figure 4: the mass deposition rate increases with supersaturation, and for the face growth rate measurements, no significant effect of solution velocity was detected. When plotted on logarithmic coordinates (not shown here) the data were correlated by

$$R_G = 9.93 \times 10^{-2} (\Delta c)^{1.61} \quad (9)$$

over the supersaturation range  $0.003 < \Delta c < 0.014$ .

The exponent on  $\Delta c$  in the overall growth measurements ( $g = 1.61$ ) lies between those of the (110) and (001) faces (1.36 and 2.04) recorded above.

#### Comparison of Face and Overall Growth Rates

The relative surface areas of the main faces were calculated from a large single crystal of nickel ammonium sulfate which gave two (001) faces of  $4.90 \times 10^{-5} \text{ m}^2$  and four (110) faces of  $5.95 \times 10^{-5} \text{ m}^2$ .

For simplicity it will be assumed that the nickel ammonium sulfate crystal is a simple parallelepiped comprising

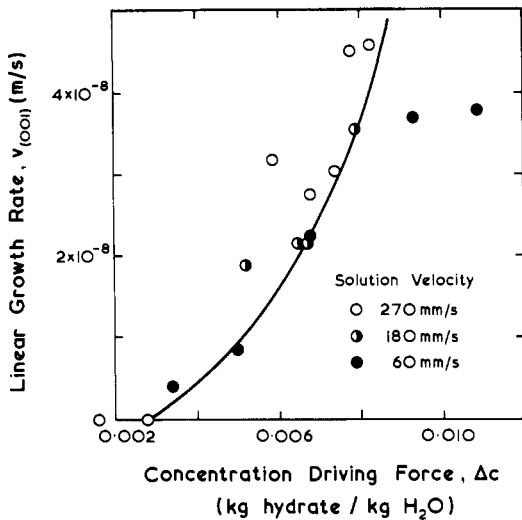


Figure 3. (001) face growth rates of nickel ammonium sulfate hexahydrate at 25°C

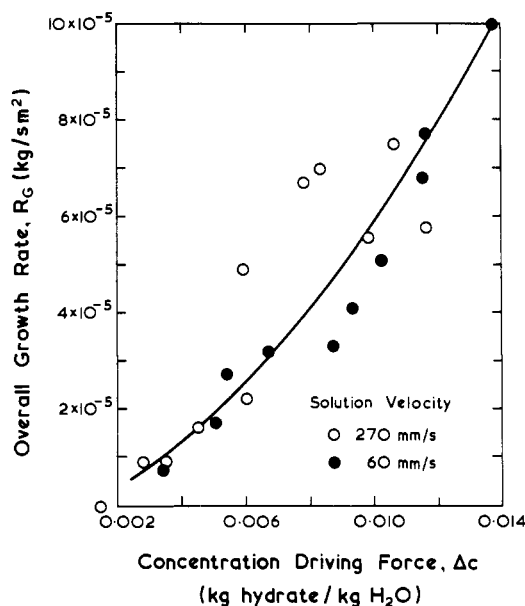


Figure 4. Overall mass deposition rates on nickel ammonium sulfate hexahydrate at 25°C, determined by weighing technique

only (110) and (001) faces. Actually, the extra area resulting from the minor faces of the crystal, i.e., the four (011) and the two (201) faces (Figure 1), adds only about 5% to the total.

The mass flux on any face ( $hkl$ ) is given by

$$R_{(hkl)} = \rho_c v_{(hkl)} \quad (10)$$

and the mass deposition rate by

$$\dot{m} = [A_{(001)}v_{(001)} + A_{(110)}v_{(110)}] \quad (11)$$

where  $A$  is the total area of all the given faces.

The overall growth rate  $R'_G$  is therefore given by

$$R'_G = \frac{[A_{(001)}v_{(001)} + A_{(110)}v_{(110)}]}{A_{(001)} + A_{(110)}} \quad (12)$$

which may be evaluated (by use of  $\rho_c = 1923 \text{ kg/m}^3$ ,  $A_{(001)} = 9.8 \times 10^{-5} \text{ m}^2$ ,  $A_{(110)} = 2.38 \times 10^{-4} \text{ m}^2$ , and  $v_{(110)}$  and  $v_{(001)}$  given by Equations 4 and 8) as

$$R'_G = 0.34 (\Delta c)^{2.04} + 0.025 (\Delta c)^{1.36} \quad (13)$$

The two parts of Equation 13 refer to the contributions of the two main groups of faces, (001) and (110), respectively. The calculated value of  $R'_G$  can then be compared with the measured value of  $R_G$ . For example, for  $\Delta c = 0.01$ , Equations 9 and 13 give

$$R_G = 6.0 \times 10^{-5} \text{ kg/sec m}^2$$

and

$$R'_G = 7.9 \times 10^{-5} \text{ kg/sec m}^2$$

This correspondence is perhaps as close as one would expect. The measured overall deposition rate is expected to be less than the calculated rate (by use of the face growth rates) because in the growth cell one of the crystal faces is attached to a wire, so the total area available for growth is less than that calculated for a complete crystal. Furthermore, when a crystal is placed in a supersaturated solution, some time has to elapse before steady-state growth conditions are achieved. Any initial time lag in the growth of the intermittently weighed crystal would, therefore, result in a measured growth rate less than that for steady-state growth. One way of overcoming this would be to weigh the crystal continuously.

On the other hand, the minor (201) and (011) faces have not been considered in calculating  $R'_G$ . Although these faces only occupy about 5% of the total surface area, they grow more rapidly than the predominant (110) and (001) faces.

#### Nomenclature

$A$  = crystal area,  $\text{m}^2$

$B$  = dimensional constant, Equation 6

$c$  = solution concentration, kg hydrated salt/kg free water

$c^*$  = equilibrium saturation concentration, kg hydrated salt/kg free water

$\Delta c$  = supersaturation,  $c - c^*$ , kg hydrated salt/kg free water

$E$  = activation energy for crystal growth, J/mol

$g$  = "order" of the crystal growth process

$hkl$  = any given crystallographic face

$K_G$  = overall mass-transfer coefficient,  $\text{kg/sec m}^2 (\Delta c)^g$

$\dot{m}$  = mass deposition rate,  $\text{kg/sec}$

$M^I$  = monovalent cation

$M^{II}$  = bivalent cation

$R$  = gas constant,  $8.314 \text{ J/mol K}$

$R_G$  = measured overall crystal growth rate,  $\text{kg/sec m}^2$

$R'_G$  = calculated overall crystal growth rate,  $\text{kg/sec m}^2$

$S$  = supersaturation,  $c/c^*$

$t$  = time, sec

$T$  = absolute temperature, K

$v$  = linear crystal growth rate,  $\text{m/sec}$

$\eta$  = solution viscosity,  $\text{N sec/m}^2$ ,  $1 \text{ cP} = 10^{-3} \text{ N sec/m}^2$

$\rho_s$  = solution density,  $\text{kg/m}^3$

$\rho_c$  = crystal density,  $\text{kg/m}^3$

#### Literature Cited

- (1) Mullin, J. W., Amatavivadhana, A., *J. Appl. Chem. London*, **17**, 151 (1967).
- (2) Mullin, J. W., "Crystallization," 2nd ed., Butterworths, London, England, 1972.
- (3) Mullin, J. W., Garside, J., *Trans. Inst. Chem. Eng. London*, **45**, 291 (1967).
- (4) Mullin, J. W., Gaska, C., *Can J. Chem. Eng.*, **47**, 483 (1969).
- (5) Mullin, J. W., Osman, M. M., *J. Chem. Eng. Data*, **12**, 516 (1967).

Received for review January 22, 1973. Accepted May 4, 1973.